






Article

Eco-Friendly Synthesis of Ni/NiO Nanoparticles Using *Gymnema sylvestre* Leaves Extract for Antifungal Activity

Manish Bhoje ¹, Shreyas Pansambal ^{2,*}, Parita Basnet ³, Kun-Yi Andrew Lin ⁴,
Karina Yanet Gutierrez-Mercado ⁵, Alejandro Pérez-Larios ^{5,*}, Ankush Chauhan ⁶, Rajeshwari Oza ¹
and Suresh Ghotekar ^{1,7,*}

- ¹ Department of Chemistry, S.N. Arts, D.J.M. Commerce & B.N.S. Science College (Autonomous), Savitribai Phule Pune University, Sangamner 422 605, India
 - ² Department of Chemistry, Shri Saibaba College, Savitribai Phule Pune University, Shirdi 423 109, India
 - ³ Department of Chemistry, Sikkim Institute of Science & Technology, Sikkim University, Gangtok 737 102, India
 - ⁴ Department of Environmental Engineering & Innovation and Development Center of Sustainable Agriculture, National Chung Hsing University, 250 Kuo-Kuang Road, Taichung 402, Taiwan
 - ⁵ Research Laboratory in Nanomaterials, Water and Energy, Engineering Department, University of Guadalajara, Campus Los Altos, Tepatitlán de Morelos 47600, Jalisco, Mexico
 - ⁶ Faculty of Allied Health Sciences, Chettinad Academy of Research and Education, Kelambakkam 603 103, India
 - ⁷ Department of Chemistry, Smt. Devkiba Mohansinhji Chauhan College of Commerce & Science, University of Mumbai, Silvassa 396 230, India
- * Correspondence: shreyas.pansambal@gmail.com (S.P.); alarios@cualtos.udg.mx (A.P.-L.); ghotekarsuresh7@gmail.com (S.G.)

Abstract: The invention of an easy synthetic approach for extremely impactful nanomaterials (NMs) is one of the crucial research areas in modern science and engineering. In the present work, we describe a cost-effective, simple, rapid and environmentally gracious biogenic fabrication of nickel/nickel oxide nanoparticles (Ni/NiO NPs) using *Gymnema sylvestre* as a natural fuel. The textural characteristics of as-prepared Ni/NiO NPs were explored using X-ray diffraction (XRD), Fourier transform infrared spectroscopy (FTIR), diffuse reflectance spectra (DRS), photoluminescence spectroscopy (PL), field-emission scanning electron microscope (FESEM), energy dispersive X-ray analysis (EDX), and high-resolution transmission electron microscopy (HRTEM). XRD affirmed the crystalline nature and phase formation of Ni/NiO NPs. The FTIR spectrum ascertains the formation of Ni/NiO NPs, and the band gap of 4.29 eV is revealed from DRS studies. Ni/NiO NPs display an intense emission peak at 576.2 nm in their PL spectrum. The fabrication of pseudo-spherical Ni/NiO NPs was displayed by FESEM and HRTEM images. The particle size obtained from HRTEM was 21 nm, which resembles the median crystallite size ascertained from the XRD data. Additionally, the plausible mechanism for Ni/NiO NPs formation is illustrated. Moreover, as-synthesized Ni/NiO NPs displayed considerable antifungal potential against *Candida albicans* and *Aspergillus niger*. Results revealed that the *Gymnema sylvestre* leaves extract can synthesize Ni/NiO NPs with appealing biological effectiveness for application in the nanomedicine sector.

Keywords: green synthesis; characterizations; Ni/NiO NPs; *Gymnema sylvestre*; antifungal efficacy



Citation: Bhoje, M.; Pansambal, S.; Basnet, P.; Lin, K.-Y.A.; Gutierrez-Mercado, K.Y.; Pérez-Larios, A.; Chauhan, A.; Oza, R.; Ghotekar, S. Eco-Friendly Synthesis of Ni/NiO Nanoparticles Using *Gymnema sylvestre* Leaves Extract for Antifungal Activity. *J. Compos. Sci.* **2023**, *7*, 105. <https://doi.org/10.3390/jcs7030105>

Academic Editor: Francesco Tornabene

Received: 29 December 2022

Revised: 14 January 2023

Accepted: 9 February 2023

Published: 7 March 2023



Copyright: © 2023 by the authors. Licensee MDPI, Basel, Switzerland. This article is an open access article distributed under the terms and conditions of the Creative Commons Attribution (CC BY) license (<https://creativecommons.org/licenses/by/4.0/>).

1. Introduction

In this swiftly developing technological era, nanotechnology has accrued a plethora of popularity owing to the invention of diverse scientific concepts to tackle the current obstacles of developing technology [1–4]. Nanomaterials' diverse applications and unique features have grabbed the interest of multiple scientific and technological concerns [5–8]. Their distinctive size, shape, area, and surface chemistry offer these features [9–12]. Moreover, the nanoscale matter differs from its micro scale counterparts in terms of several characteristics such

as electro-optical, chemical, magneto-optical, mechanical, and surface-area-to-volume ratio [13–15]. Therefore, such properties of nanomaterials make them enormously aggressive and more enticing for scientists [16–20]. As a result, nanomaterial offers splendid uses in various sectors like medicine, solar cells, energy, defense, catalysis, agriculture, textiles, cosmetics, sensors, ceramics, drug delivery, environment, food industry, and many more.

Bacterial growth and proliferation can happen anywhere, and bacterial infections are a severe health problem for living things. There is a great demand for effective antimicrobial drugs since bacterial infectious illnesses result in significant morbidity and death [21,22]. NPs made using a green method have shown potential efficacy in this field [23]. The ability of bacteria to live and create various infections under varying circumstances is a result of their exposure to various environmental fluctuations, including temperature, molarity, radiation, toxins, and restricted nourishment. As a result, bacterial resistance to antibiotic therapy is becoming a significant clinical and public health issue globally. Inappropriate use of antibiotics and a lack of innovative approaches to the development of antibacterial agents are the main causes of antimicrobial resistance [24,25]. Additionally, it is anticipated that by 2050, antibiotic resistance will become a global epidemic with 10 million fatalities [26]. Therefore, proper actions and practices are essential to address the problem of microbial resistance. Different mechanisms, such as altered binding target sites, enzyme synthesis, influx and efflux mechanisms, etc., might cause bacteria to become resistant to therapies. To solve this problem, new antimicrobial compounds were required [27–30]. Numerous antimicrobial NPs (metal, metalloid, metal oxides, spinels, perovskites, etc.) have demonstrated their efficacy in vitro, on animal cells, and against infectious illnesses [31,32]. The type of bacterial species and the metal oxide NPs being used affect antimicrobial action.

Nickel (Ni) and nickel oxide (NiO) NPs are of fantastic prominence due to their peculiar catalytic, unusual electronic, and spectacular magnetic characteristics [33,34]. Ni metal belongs to the first transition series that possesses magnetic and catalytic and hydrogen storage abilities [35]. Moreover, Ni is a strong option for use in biomedicine, magnetism, electronics, and energy technology due to its eco-benevolent aspect and excellent reactivity [36–38]. The environmental benefits of Ni NPs in the sector of adsorption of inorganic contaminants and toxic dyes are crucial to maintaining a clean environment [39,40]. Due to their efficacious anti-inflammatory and antibacterial properties, they have been applied in biomedicines [37]. Moreover, its oxide, NiO, is a p-type semiconductor with a cubic lattice structure with a large band gap between 3.6 and 4.0 eV [41]. These NPs are being explored meticulously and earned considerable popularity due to their excellent chemical stability and super-capacitive and electro-catalytic features [42–44]. Moreover, NiO NPs offer promising applications in fuel cells, catalysis, electrochromic films, magnetic materials, gas sensors, battery cathodes, optical fibers, etc., [33,34]. Due to minimal material cost, volume effect, surface effect, macroscopic tunnel effect, and quantum size effect, Ni and NiO NPs are immensely inspiring topics in the contemporary realm of research [45].

To date, numerous traditional chemical and physical approaches have been reported for producing Ni/NiO NPs [33,34,46]. These fabrication approaches are commonly expensive, labor-intensive, and time-consuming and may harm the ecosystem and living things. Thus, “*Green Synthesis*”, an alternative approach for manufacturing NPs that is affordable, rapid, efficient, and environmentally sustainable, was invented [47,48]. The key features of the green synthesis approach are the careful planning of the synthesis, non-noxious precursors, and benign reaction conditions to mitigate or remove the negative impacts [49,50]. Moreover, a green approach uses biological components, such as algae, bacteria, plants, fungi, bio-polymers, and bio-waste materials, as natural reductants and stabilizers [51–53]. However, due to their higher rate of reduction, ease of availability, sustainability, and abundance of biologically active compounds, plants are seen to be the most viable alternative [54,55]. Furthermore, the concentration of plant extract, metal precursors, pH, temperature, and reaction time all affect the effectiveness of green technologies. The secondary metabolites found in the plant extract are important in reducing metal ions to metal/metal oxide NPs. The plant extract’s phytoconstituents include

alkaloids, tannins, flavonoids, glycosides, terpenoids, steroids, amino acids, volatile oils, organic acids, alcohols, saponins, polyphenols, vitamins, and carbohydrates as the numerous functional groups, are what create the nanoparticles' reducing and capping/stabilizing properties. Such functional groups act as a capping moiety to NPs, stabilizing them and preventing agglomeration.

Amidst potential therapeutic plants, *Gymnema sylvestre*, a member of the Apocynaceae family, has historically been prescribed to cure several diseases [56]. It is a wild herb found in Africa, China, India, and Australia. Due to its potency in treating severe illnesses such as cancer, asthma, cardiovascular disease, diabetes, and obesity, diverse formulations of this plant are observed in several products, namely food supplements, health tablets, and tea bags [56,57]. In diverse reports, the presence of biologically active compounds in *Gymnema sylvestre* is claimed to be effective against anemia, diuretic, arthritis, hypercholesterolemia, indigestion, osteoporosis, asthma, cardiopathy, microbial infections, constipation, and as an anti-inflammatory agent [58]. As depicted in Figure 1, *Gymnema sylvestre* extract possesses diverse biologically active molecules, namely gymnestrogenin, gymnemanol, lupeol, quercitol, conduritol A, paraben, d-quercitol, stigmasterol, and gymnemic acid-I, etc., [56].

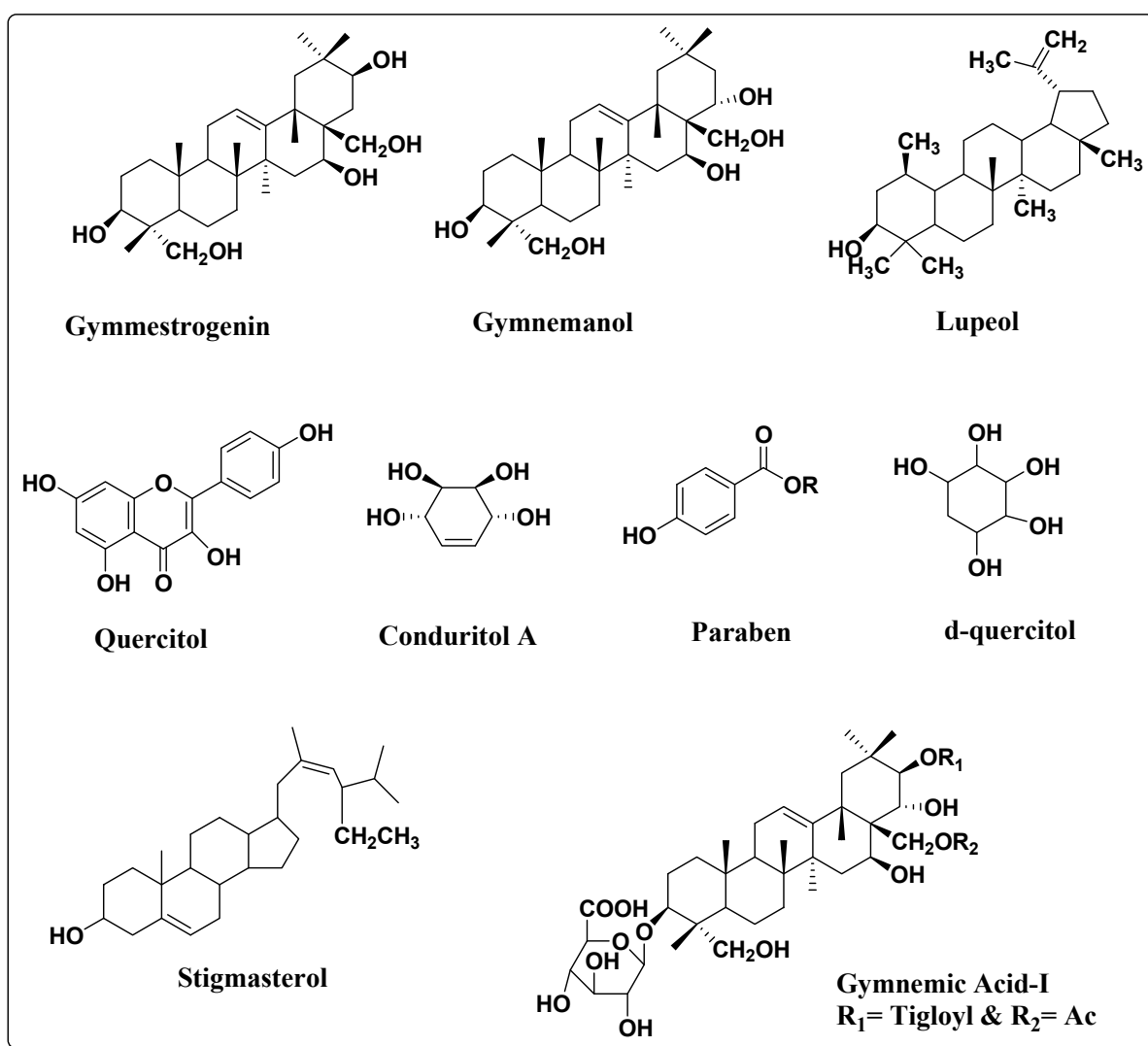


Figure 1. Phytochemical constituents in *Gymnema sylvestre*.

In view of this, present study demonstrate an inexpensive, facile, green, and environmentally benevolent approach to synthesize Ni/NiO NPs employing leaves extract of *Gymnema sylvestre* as natural reducing and capping agent. Moreover, the characteristic

properties (using XRD, FTIR, DRS, PL, FESEM, EDX, and HRTEM analysis) and antifungal activity of as-synthesized Ni/NiO NPs have been studied extensively.

2. Materials and Methods

2.1. Preparation of Extract from *Gymnema sylvestre* Leaves

Fresh leaves of *Gymnema sylvestre* were sourced from the Bhimashankar region, Pune, Maharashtra, India. These collected leaves of *Gymnema sylvestre* were carefully rinsed with double distilled water (ddH₂O) to eliminate any surface dust/debris and then shade-dried at room temperature (RT). After drying, the leaves were finely ground using a domestic blender. Then, 2 g of fine powder of leaves was poured into a 250 mL beaker containing 100 mL of ddH₂O and boiled at 80–90 °C for 20 min. The resulting solution was filtered through filter paper (Whatman filter paper no. 1) and placed at 4 °C until the further synthesis work of NPs.

2.2. Biosynthesis of Ni/NiO NPs

For the biogenic synthesis of Ni/NiO NPs, nickel nitrate (Ni(NO₃)₂·6H₂O, 99%, SRL Chem.) was used as a metal precursor. A total of 5 mL of leaves extract of *Gymnema sylvestre* was mixed drop-wise to freshly prepared 0.1 M nickel nitrate under continuous stirring using a magnetic stirrer for 25 min at 500 rpm. Then, the color of the resultant solution changed from greenish to yellowish green. Next, the solution was centrifuged, and the residue was calcined in a muffle furnace at 400 °C for 2 h. A fine black-colored material was obtained, carefully collected, and stored for further study.

2.3. Analytical Tools for Characterization

The green synthesis of Ni/NiO NPs using leaves extract of *Gymnema sylvestre* was confirmed using various physical characterization tools. The crystallographic elucidation of Ni/NiO NPs was accomplished by X-ray diffraction (XRD, Bruker, D8-Advanced Diffractometer, Germany) profile with Cu-K α radiation ($\lambda = 0.154$ nm). The functional group assessment of as-synthesized Ni/NiO NPs was performed using FTIR-4600 typeA. The absorption and optical characteristics of Ni/NiO NPs were scrutinized using Jasco Spectrophotometer V-770 and JOBIN–YVON FLUROLOG-3-11 Spectrofluorimeter. The textural properties, including the size and topology of Ni/NiO NPs were investigated through field emission scanning electron microscopy (FESEM, Nova NanoSEM NPEP303, Japan) and transmission electron microscopic (TEM, PHILIPS CM200, Japan). The elemental composition and chemical purity were revealed by energy dispersive X-ray spectroscopy (EDX, Bruker, XFlash 6I30, Japan).

2.4. Antifungal Activity of Biosynthesized Ni/NiO NPs

The antifungal activity of greenly produced Ni/NiO NPs was screened by using the agar well diffusion assay against two fungal pathogens, namely *Candida albicans* (NCIM 3100) and *Aspergillus niger* (ATCC 504). The suspension of Ni/NiO NPs at a concentration of 1 mg/mL was produced and used for further experimental work. For the growth of fungi, Mueller-Hinton agar media was prepared, autoclaved, and allowed to solidify. The fungal cultures were eventually distributed using sterile cotton swabs on Mueller-Hinton agar plates. Five millimeter wells were then created with a cork borer and filled with Ni/NiO NPs of the same concentration (1 mg/mL). Fluconazole (1 mg/mL) was applied as the reference (positive control). The radius of each well was ascertained to be an inhibitory zone and estimated in mm via Vernier caliper after 48 h of incubation at 37 °C.

3. Results and Discussion

3.1. Structural Elucidation Using XRD Profile

In the biosynthesis of NPs, particularly of metal oxide NPs, it has been reported in several studies that not all metal NPs convert into metal oxides; instead, the formation of a double phase of metal-metal oxide NPs is observed in most of the cases [59–61]. In

this work, wherein the green fabrication of NPs was performed using the leaves extract of *Gymnema sylvestre*, the formation of a single phase of NiO or double phase of Ni-NiO NPs was identified through the X-ray diffraction (XRD) analysis. Figure 2 represents the XRD spectra of the as-synthesized NPs. From the spectrum, strong and narrow diffraction peaks may be noticed, which evinces the high crystallinity of the as-synthesized Ni/NiO NPs. The diffraction peaks were noticed at diffraction angles corresponding to the reflection peaks belonging to the (*hkl*) values of (111), (200), (111), (200), and (111) (as marked in Figure 2), respectively. It may be observed from Figure 2 that two phases have formed, marked by (*) for the NiO phase and (#) for the Ni phase. The diffraction peaks belonging to NiO NPs are comparatively sharp, indicating the dominance of this phase over the Ni NPs phase. It is important to mention here that in the process of biosynthesis using plant extracts, the plant extract is used as both the capping and reducing agent; therefore, no chemical hydroxide sources such as NaOH, NH₄OH, etc., are used. Thus, for the complete conversion of Ni-metal precursor into NiO NPs, the calcination temperature must be able to convert all the reduced Ni NPs into their respective oxide. It has been reported by Garcia-Cerda et al. [62] that in the case of NiO NPs, only one phase of NiO NPs was obtained when the calcination temperature was kept at 600 °C for 2 h duration. In this work, the calcination temperature was maintained at 400 °C for 2 h. This was done to prevent the bio-capped plant phytochemicals from decomposing completely. Therefore, two phases were observed in the XRD spectra of NPs corresponding to Ni NPs and NiO NPs. Any other phase signifying the presence of impurities was not observed. Using Scherrer's equation, the median crystallite size of Ni/NiO NPs was estimated to be 25 nm. The plant extract can serve as a fuel and a capping agent, so reducing the particle size, so the method used may be responsible for the smaller crystallites. Consequently, the biologically produced Ni/NiO NP's small crystallite size and high crystallinity will notably influence the biological functioning of the NPs.

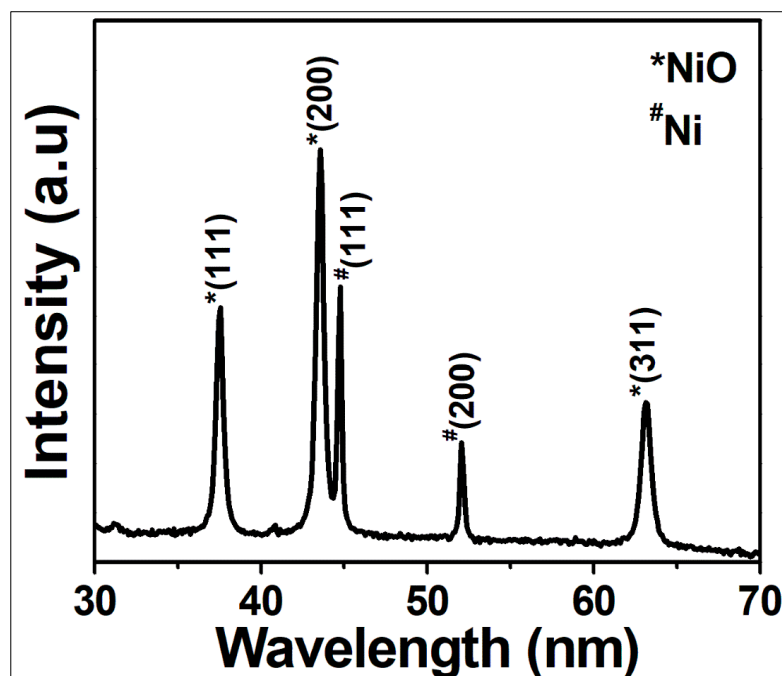


Figure 2. XRD spectrum of *Gymnema sylvestre* leaves extract mediated biosynthesized Ni/NiO NPs.

3.2. Vibrational Properties

The important phytochemical functional groups of *Gymnema sylvestre* present in the biosynthesized Ni/NiO NPs were identified using the Fourier transform infra-red (FTIR) spectra. These phytochemicals are the possible reducing and capping agents in the biosynthesis of Ni/NiO NPs. The FTIR spectrum of Ni/NiO NPs is shown in Figure 3. The promi-

ment bands have been marked in Figure 3, which was observed at 3430 cm^{-1} , 2915 cm^{-1} , 1630 cm^{-1} , 1384 cm^{-1} , and 1017 cm^{-1} . The strong band observed at 3430 cm^{-1} corresponds to the symmetrical stretching vibrations of -OH groups of the hydroxyl molecule [63]. The transmittance band observed at 2915 cm^{-1} may be assigned to the C-H bond stretching. The band at 1630 cm^{-1} may be ascribed to the O-H deformation of water adsorbed at the surface of the as-prepared Ni/NiO NPs or to the C=O stretching vibrations. Likewise, the carbonyl stretching band was observed at 1384 cm^{-1} . Finally, the band appearing at 1017 cm^{-1} represents the C-N stretching vibration of aromatic and aliphatic amines, which may be further ascribed to the existence of complex phenolic structures [63]. Further, some low-lying bands were also observed at 2848 cm^{-1} , 1744 cm^{-1} , and 1456 cm^{-1} . These bands may be ascribed to $-\text{CH}_2$ vibrations of aliphatic hydrocarbons [64], carboxylic groups from dimerized saturated aliphatic acids [65], and C=C aromatic ring stretching vibrations, respectively. Therefore, the phytochemical moieties of the plant extract obtained in the FTIR spectra, mainly phenolic groups, flavones, tannins, and aliphatic acids, were accountable for reducing the metal precursor. At the same time, the residues acted as the capping agent. Furthermore, no other impurity phase was identified, and the results of the FTIR spectrum of biologically fabricated Ni/NiO NPs were in perfect concordance with those of the XRD results.

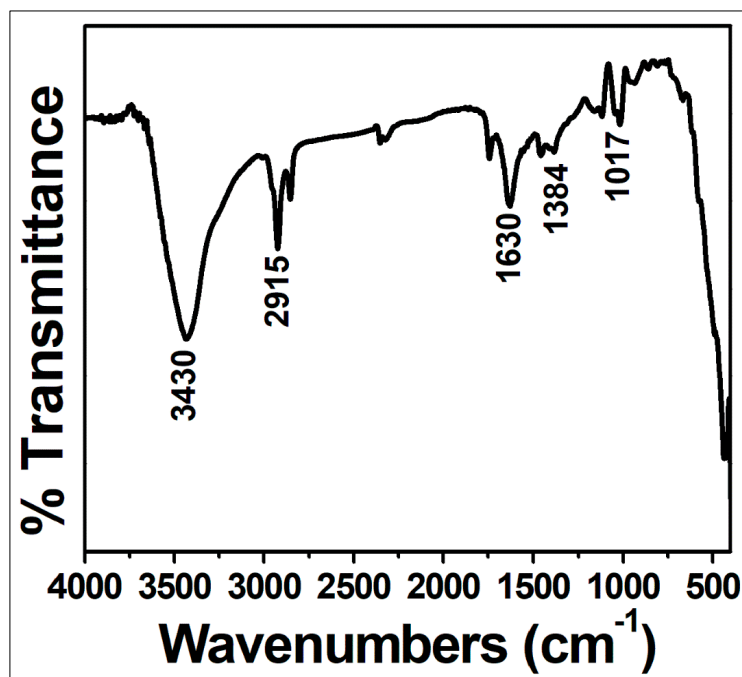


Figure 3. FTIR spectrum of biologically fabricated Ni/NiO NPs using leaves extract of *Gymnema sylvestre*.

Figure 4 depicts the main active biomolecules (Figure 1) found in *Gymnema sylvestre* extracts in order to explain how the metal precursor salt $\text{Ni}(\text{NO}_3)_2 \cdot 6\text{H}_2\text{O}$ can change into Ni/NiO NPs. The proposed reaction mechanism demonstrates how diverse biological molecules behave as stabilizing and reducing agents. Different active biomolecules found in *Gymnema sylvestre* include gymnestrogenin, gymnemanol, lupeol, quercitol, conduritol A, paraben, d-quercitol, stigmaterol, and gymnemic acid-I. However, gymnemanol has been selected as a sample molecule for the mechanism. Because the hydroxyl groups adhere to nickel ions, nickel and gymnemanol form a stable complex. After calcination, the complex decomposes and produces Ni/NiO NPs. This was done to prevent the bio-capped plant phytochemicals from decomposing completely. As a result, the formation of Ni and NiO is not selective. Therefore, two phases were observed in the XRD analysis corresponding to Ni NPs and NiO NPs.

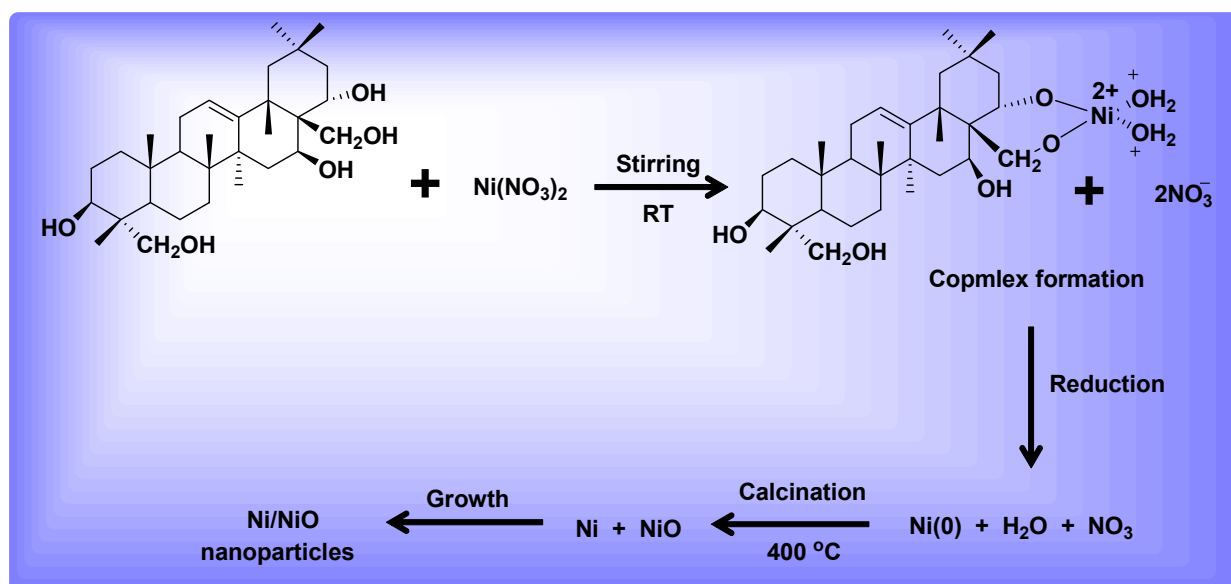


Figure 4. A possible reaction mechanism for the green synthesis of Ni/NiO NPs using biomolecules.

3.3. UV-Visible Analysis

The UV-Vis absorption spectrum of the as-prepared Ni/NiO NPs is depicted in Figure 5. The biologically synthesized Ni/NiO NPs annealed at 400 °C evinced a high absorption band in the UV range; therefore, it could absorb maximum UV radiation. A very strong absorption band was observed at 288.9 nm. This absorption band may be attributed to the essential band-gap attraction of Ni/NiO NPs due to the electronic transitions from the valence band to the conduction band, i.e., O 2p to Ni 3d [66]. Therefore, the strong absorption band in this area is the outcome of ligand-to-metal charge transfer (LMCT) direct transition [66]. The band gap energy was ascertained using Planck's equation and was found to be 4.29 eV. This implies that the as-synthesized Ni/NiO NPs are a visible light active material.

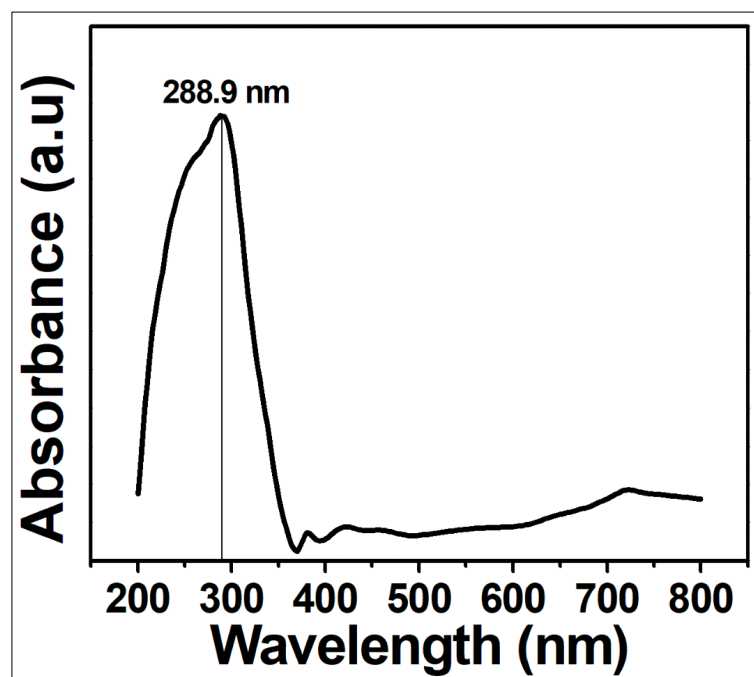


Figure 5. UV-visible spectrum of biosynthesized Ni/NiO NPs using leaves extract of *Gymnema sylvestre*.

3.4. PL Analysis

It is a well-known fact that in the case of metal oxide NPs, the photoluminescence (PL) emission may be categorized into two specific types, namely, near band edge (NBE) emission and deep level (DL) emission. The former refers to the emissions in the UV region due to excitonic recombination, while the latter accounts for the radiative recombination of a photo-generated hole with an electron occupying the oxygen vacancy [67].

The PL spectrum of the as-synthesized Ni/NiO NPs is depicted in Figure 6. It may be observed that the PL spectrum of Ni/NiO NPs is dominated by the defect-related deep-level emissions (DLE) in the visible (green) region and no peaks pertaining to the excitonic recombination or other visible-region peaks may be observed. This implies that the as-synthesized Ni/NiO NPs have minimum defect states in-relation to the non-existence of defect-related emissions other than the green emission at 576.2 nm. This intense green emission band (or DLE) may be attributed to the nickel vacancies; however, the possibility of its origin as a result of oxygen vacancies cannot be ruled out [68]. Furthermore, these vacancies also indicate the charge transfer between Ni^{2+} and Ni^{3+} species thereby confirming their presence in the NiO lattice [68]. Hence, the greenly fabricated Ni/NiO NP's intrinsic structural defects suggest it can boost biological activities.

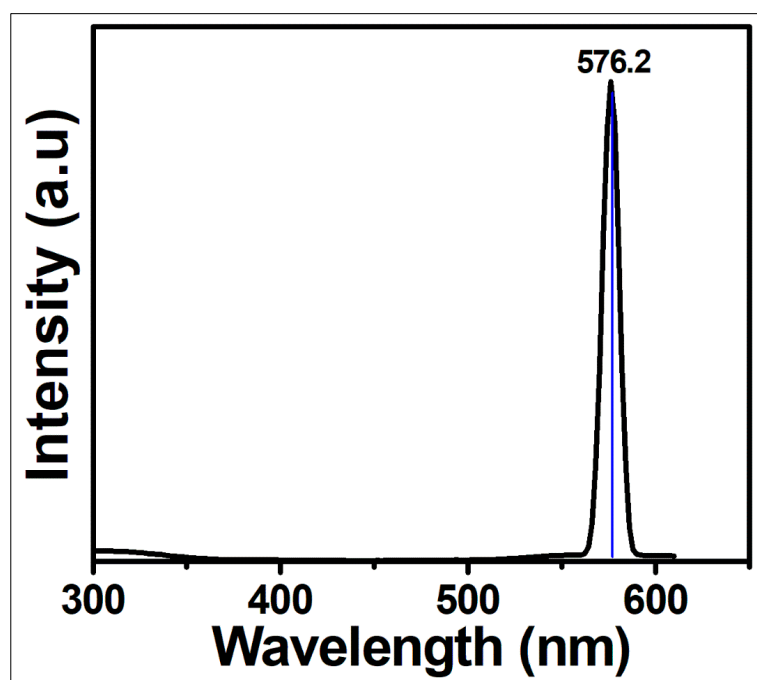


Figure 6. PL spectrum of greenly synthesized Ni/NiO NPs using leaves extract of *Gymnema sylvestre*.

3.5. SEM and EDX Analysis

The morphology of any metal oxide NPs is an important parameter that decides the properties related to its surface activity. Considering this, the morphology of the biosynthesized Ni/NiO NPs was characterized through the scanning electron microscopy (SEM) technique, and the result is presented in Figure 7a. It may be observed from this image that the particles do not have a fixed morphology, wherein some particles assume an oval shape while most of the other particles have a pseudo-spherical shape.

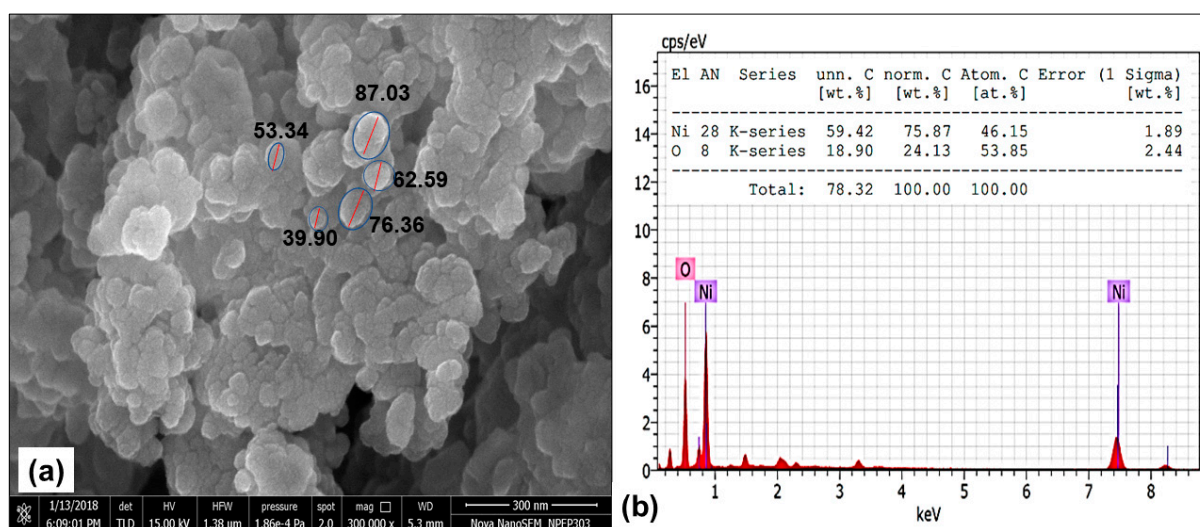


Figure 7. (a) SEM image, and (b) EDX graph of the biologically fabricated Ni/NiO NPs using leaves extract of *Gymnema sylvestre*.

This implies that the amount of the bio-extract used was insufficient to impart particles a common morphology (as may be observed from the figure). Nevertheless, authors obtained nano-sized Ni/NiO NPs with particle sizes of 60–65 nm through this biosynthesis technique. Figure 7b depicts the elemental composition of the as-synthesized Ni/NiO NPs based on the energy dispersive X-ray (EDX) technique. From this figure, the presence of Ni and O in the sample is evident. Furthermore, the weak unassigned peaks belong to C, Al, and K, which may be attributed to the presence of plant phytochemicals in the sample.

3.6. HRTEM and SAED Pattern Analysis

The microstructural analysis of the as-synthesized Ni/NiO NPs was performed through the transmission electron microscopy (TEM) technique. Figure 8a corresponds to the TEM image of Ni/NiO NPs, and Figure 8b depicts its selected area electron diffraction (SAED) pattern. The TEM image shows that most particles have pseudo-spherical structures similar to their morphology (Figure 7a). Further, the size of the particles was in the range of 12 nm (smallest) to 28 nm (largest), while the mean particle size was ascertained to be ~21 nm. SAED pattern reveals the crystallinity or amorphous nature of a material. The SAED pattern represented in Figure 8b for Ni/NiO NPs shows the existence of bright-colored spots in the form of concentric circles. Hence, this pattern indicated the polycrystalline nature of the as-synthesized Ni/NiO NPs. Because of their high dispersity, small particle size, and high specific surface area, greenly produced Ni/NiO NPs are a potential material for biological applications.

3.7. Antifungal Efficacy of Ni/NiO NPs

The as-prepared Ni/NiO NPs were evaluated for their antifungal performance using flucanazole as a control (Figure 9). The results of a zone of inhibition (mm) values are compiled in Table 1. The greenly produced Ni/NiO NPs displayed considerable antifungal potential against *Candida albicans* and *Aspergillus niger* (Figure 8). The highest efficacy was displayed against *C. albicans* with an inhibition zone of 22.2 mm at a volume of 1 mg/mL Ni/NiO NPs suspension. At the same time, Ni/NiO NPs displayed considerable inhibition performance against *A. niger* with an inhibition zone of 18.8 mm. Similar results were reported in the study by Suresh et al. [69] when *A. niger* was subjected to an antifungal assay using biogenically produced NiO NPs. Moreover, *A. niger* was the target of NiO NPs powerful antifungal action, according to Ahmad et al. [70].

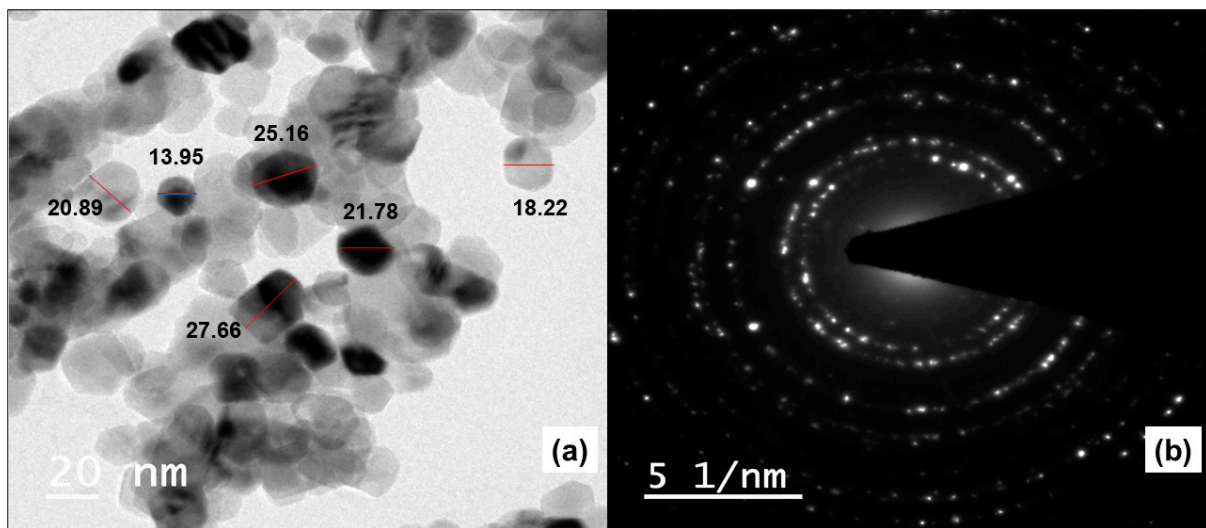


Figure 8. (a) TEM image, and (b) SAED pattern of the greenly synthesized Ni/NiO NPs.

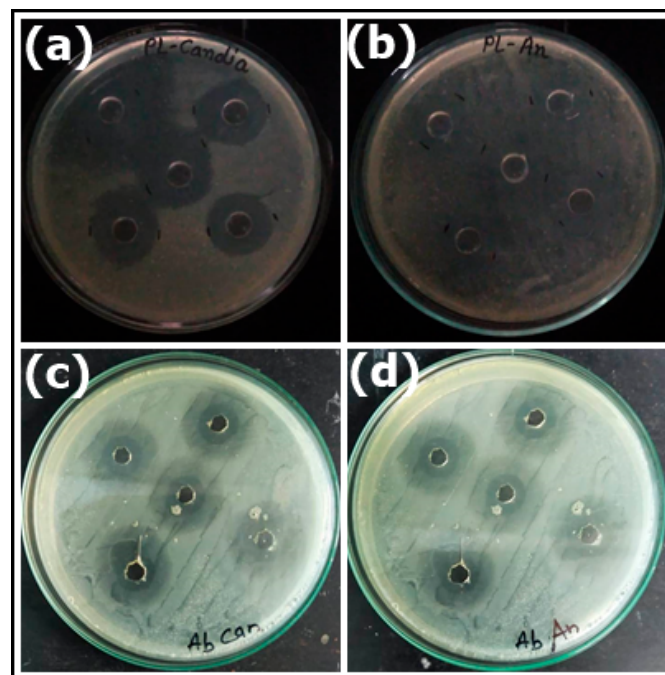


Figure 9. Antifungal effect of biologically synthesized Ni/NiO NPs against (a) *Candida albicans* (b) *Aspergillus niger* and comparative effect of fluconazole (control) against (c) *Candida albicans* (d) *Aspergillus niger*.

Table 1. Antifungal effect of biogenically produced Ni/NiO NPs using leaves extract of *Gymnema sylvestre*.

Entry	Fungal Strain	Average Zone of Inhibition (mm)	
		Ni/NiO NPs	Fluconazole
1	<i>Candida albicans</i> (NCIM 3100)	22.2	28
2	<i>Aspergillus niger</i> (ATCC504)	18.8	30

The Ni/NiO NPs facilitate dispersibility and allow the interaction of extracellular Ni²⁺ with intracellular Ca²⁺ metabolism, which causes cell damage. When the size of the NPs decreases, the electrostatic interaction between the microbial cell membrane and Ni ions

released from Ni/NiO NPs becomes strong. It hence increases the fungicidal efficacy [71]. The activity also depends on the physicochemical properties of the NPs for long-term performance. In general, the particle dosage, methodology, and duration of treatment all affect how effectively a potential antimicrobial works [72].

Also, the electrostatic interaction between the positively charged nickel ions (Ni^{2+}) and the negatively charged bacterial cell membranes may regulate the antifungal activity of the produced Ni/NiO NPs. The Ni/NiO NPs emit Ni^{2+} , which enters the cell wall and damages the DNA, mitochondria, proteins, and electron transport, ultimately leading to cell death. Protein leakage results from Ni/NiO NPs diffusion and buildup in the cell membrane, which changes membrane permeability.

According to the mechanism mentioned above and investigations, the biologically fabricated Ni/NiO NPs using leaves extract of *Gymnema sylvestre* have effective antifungal characteristics and can be administered at the appropriate dose to target a particular microbe or afflicted tissue with minimal side effects.

4. Conclusions

In the present study, the Ni/NiO NPs were successfully fabricated via green synthesis and one-pot technique using leaves extract of *Gymnema sylvestre* for antifungal studies. Crystallographic structure, chemical composition, and textural properties of the fabricated Ni/NiO NPs were investigated through XRD, FTIR, UV-DRS, PL, FESEM, EDX, and HRTEM analyses, respectively. The initial analysis confirmed the production of Ni/NiO NPs with a mean size of 25 nm and a pseudo-spherical morphology. XRD and FTIR studies affirmed the phase formation of Ni/NiO NPs. The intense peaks reveal the high crystalline nature of the Ni/NiO NPs, and the sharp PL emission at 576.2 nm affirms the existence of the defect states, which are accountable for their good antifungal performance. The green synthesized Ni/NiO NPs possess good antifungal performance by the action of UV and visible light, which contributes to generating electron-hole pairs, thereby forming hydrogen peroxide (H_2O_2), which penetrates the cell membrane and destroys bacteria. Moreover, as-prepared Ni/NiO NPs displayed considerable antifungal performance against *Candida albicans* and *Aspergillus niger*. The result of the zone of inhibition proves that the fabricated Ni/NiO NPs show a considerable antifungal performance and were found to be potent against fungal strains. Based on this work, it is conceivable to consider green synthesized Ni/NiO NPs as a potential alternative for antimicrobial agents that could deal with the major emerging obstacle of antibiotics. Hence the biologically fabricated Ni/NiO NPs can be employed as antimicrobial coatings for environmental and biomedical uses.

Author Contributions: Conceptualization, M.B. and S.P.; methodology, S.P.; investigation, S.P. and S.G.; data curation, P.B., A.C. and K.-Y.A.L.; writing—original draft preparation, P.B. and S.G.; writing—review and editing, K.Y.G.-M., A.P.-L. and S.G.; supervision, R.O. All authors have read and agreed to the published version of the manuscript.

Funding: This research received no external funding.

Data Availability Statement: Not applicable.

Acknowledgments: Authors are grateful to SAIF-IIT Bombay and CIF-Savitribai Phule Pune University, Pune for providing the characterization facilities.

Conflicts of Interest: The authors declare no conflict of interest.

References

1. Lu, J.; Chen, Z.; Ma, Z.; Pan, F.; Curtiss, L.A.; Amine, K. The role of nanotechnology in the development of battery materials for electric vehicles. *Nat. Nanotechnol.* **2016**, *11*, 1031–1038. [[CrossRef](#)] [[PubMed](#)]
2. Lowry, G.V.; Avellan, A.; Gilbertson, L.M. Opportunities and challenges for nanotechnology in the agri-tech revolution. *Nat. Nanotechnol.* **2019**, *14*, 517–522. [[CrossRef](#)] [[PubMed](#)]
3. Cuong, H.N.; Pansambal, S.; Ghotekar, S.; Oza, R.; Hai, N.T.T.; Viet, N.M.; Nguyen, V.-H. New frontiers in the plant extract mediated biosynthesis of copper oxide (CuO) nanoparticles and their potential applications: A review. *Environ. Res.* **2022**, *203*, 111858. [[CrossRef](#)] [[PubMed](#)]

4. Kumar, P.; Mahajan, P.; Kaur, R.; Gautam, S. Nanotechnology and its challenges in the food sector: A review. *Mater. Today Chem.* **2020**, *17*, 100332. [[CrossRef](#)]
5. Pansambal, S.; Oza, R.; Borgave, S.; Chauhan, A.; Bardapurkar, P.; Vyas, S.; Ghotekar, S. Bioengineered cerium oxide (CeO₂) nanoparticles and their diverse applications: A review. *Appl. Nanosci.* **2022**, 1–26. [[CrossRef](#)]
6. Harish, V.; Tewari, D.; Gaur, M.; Yadav, A.B.; Swaroop, S.; Bechelany, M.; Barhoum, A. Review on nanoparticles and nanostructured materials: Bioimaging, biosensing, drug delivery, tissue engineering, antimicrobial, and agro-food applications. *Nanomaterials* **2022**, *12*, 457. [[CrossRef](#)]
7. Ghotekar, S.; Pansambal, S.; Lin, K.-Y.A.; Pore, D.; Oza, R. Recent Advances in Synthesis of CeVO₄ Nanoparticles and Their Potential Scaffold for Photocatalytic Applications. *Top. Catal.* **2022**, *66*, 89–103. [[CrossRef](#)]
8. Sharmiladevi, P.; Girigoswami, K.; Haribabu, V.; Girigoswami, A. Nano-enabled theranostics for cancer. *Mater. Adv.* **2021**, *2*, 2876–2891. [[CrossRef](#)]
9. Gawande, M.B.; Goswami, A.; Felpin, F.-X.; Asefa, T.; Huang, X.; Silva, R.; Zou, X.; Zboril, R.; Varma, R.S. Cu and Cu-based Nanoparticles: Synthesis and Applications in Catalysis. *Chem. Rev.* **2016**, *116*, 3722–3811. [[CrossRef](#)]
10. Gawande, M.B.; Goswami, A.; Asefa, T.; Guo, H.; Biradar, A.V.; Peng, D.-L.; Zboril, R.; Varma, R.S. Core-shell nanoparticles: Synthesis and applications in catalysis and electrocatalysis. *Chem. Soc. Rev.* **2015**, *44*, 7540–7590. [[CrossRef](#)]
11. Kashid, Y.; Ghotekar, S.; Bilal, M.; Pansambal, S.; Oza, R.; Varma, R.S.; Nguyen, V.-H.; Murthy, H.A.; Mane, D. Bio-inspired sustainable synthesis of silver chloride nanoparticles and their prominent applications. *J. Indian Chem. Soc.* **2022**, *99*, 100335. [[CrossRef](#)]
12. Ghosh, D.; Sarkar, D.; Girigoswami, A.; Chattopadhyay, N. A fully standardized method of synthesis of gold nanoparticles of desired dimension in the range 15 nm–60 nm. *J. Nanosci. Nanotechnol.* **2011**, *11*, 1141–1146. [[CrossRef](#)]
13. Rahman, S.; Lu, Y. Nano-engineering and nano-manufacturing in 2D materials: Marvels of nanotechnology. *Nanoscale Horiz.* **2022**, *7*, 849–872. [[CrossRef](#)]
14. Fan, W.; Yung, B.; Huang, P.; Chen, X. Nanotechnology for multimodal synergistic cancer therapy. *Chem. Rev.* **2017**, *117*, 13566–13638. [[CrossRef](#)]
15. Korde, P.; Ghotekar, S.; Pagar, T.; Pansambal, S.; Oza, R.; Mane, D. Plant extract assisted eco-benevolent synthesis of selenium nanoparticles—a review on plant parts involved, characterization and their recent applications. *J. Chem. Rev.* **2020**, *2*, 157–168.
16. Ribeiro, A.I.; Dias, A.M.; Zille, A. Synergistic effects between metal nanoparticles and commercial antimicrobial agents: A review. *ACS Appl. Nano Mater.* **2022**, *5*, 3030–3064. [[CrossRef](#)]
17. Maksoud, M.I.A.A.; Fahim, R.A.; Bedir, A.G.; Osman, A.I.; Abouelela, M.M.; El-Sayyad, G.S.; Elkodous, M.A.; Mahmoud, A.S.; Rabee, M.M.; Al-Muhtaseb, A.H.; et al. Engineered magnetic oxides nanoparticles as efficient sorbents for wastewater remediation: A review. *Environ. Chem. Lett.* **2022**, *20*, 519–562. [[CrossRef](#)]
18. Chauhan, G.; González-González, R.B.; Iqbal, H.M. Bioremediation and decontamination potentials of metallic nanoparticles loaded nanohybrid matrices—A review. *Environ. Res.* **2022**, *204*, 112407. [[CrossRef](#)]
19. Ghotekar, S.; Pansambal, S.; Nguyen, V.-H.; Bangale, S.; Lin, K.-Y.A.; Murthy, H.C.A.; Oza, R. Spinel ZnCr₂O₄ nanorods synthesized by facile sol-gel auto combustion method with biomedical properties. *J. Sol-Gel Sci. Technol.* **2022**, *105*, 176–185. [[CrossRef](#)]
20. Limón-Rocha, I.; Marizcal-Barba, A.; Guzmán-González, C.A.; Anaya-Esparza, L.M.; Ghotekar, S.; González-Vargas, O.A.; Pérez-Larios, A. Co, Cu, Fe, and Ni Deposited over TiO₂ and Their Photocatalytic Activity in the Degradation of 2, 4-Dichlorophenol and 2, 4-Dichlorophenoxyacetic Acid. *Inorganics* **2022**, *10*, 157. [[CrossRef](#)]
21. Khan, S.T.; Musarrat, J.; Al-Khedhairi, A.A. Countering drug resistance, infectious diseases, and sepsis using metal and metal oxides nanoparticles: Current status. *Colloids Surf. B Biointerfaces* **2016**, *146*, 70–83. [[CrossRef](#)] [[PubMed](#)]
22. Cohen, M.L. Changing patterns of infectious disease. *Nature* **2000**, *406*, 762–767. [[CrossRef](#)] [[PubMed](#)]
23. Samiei, M.; Farjami, A.; Dizaj, S.M.; Lotfipour, F. Nanoparticles for antimicrobial purposes in Endodontics: A systematic review of in vitro studies. *Mater. Sci. Eng. C* **2016**, *58*, 1269–1278. [[CrossRef](#)] [[PubMed](#)]
24. Cantón, R.; Horcajada, J.P.; Oliver, A.; Garbajosa, P.R.; Vila, J. Inappropriate use of antibiotics in hospitals: The complex relationship between antibiotic use and antimicrobial resistance. *Enferm. Infecc. Microbiol. Clin.* **2013**, *31*, 3–11. [[CrossRef](#)] [[PubMed](#)]
25. Tangcharoensathien, V.; Chanvatik, S.; Sommanustweechai, A. Complex determinants of inappropriate use of antibiotics. *Bull. World Health Organ.* **2018**, *96*, 141–144. [[CrossRef](#)] [[PubMed](#)]
26. Sugden, R.; Kelly, R.; Davies, S. Combatting antimicrobial resistance globally. *Nat. Microbiol.* **2016**, *1*, 16187. [[CrossRef](#)]
27. Pourmadadi, M.; Rahmani, E.; Eshaghi, M.M.; Shamsabadipour, A.; Ghotekar, S.; Rahdar, A.; Ferreira, L.F.R. Graphitic carbon nitride (g-C₃N₄) as a new carrier for drug delivery applications: A review. *J. Drug Delivery Sci. Technol.* **2022**, *79*, 104001. [[CrossRef](#)]
28. Pourmadadi, M.; Ostovar, S.; Eshaghi, M.M.; Rajabzadeh-Khosroshahi, M.; Safakhah, S.; Ghotekar, S.; Rahdar, A.; Díez-Pascual, A.M. Nanoscale MOFs as an advanced tool for medical applications: Challenges and recent progress. *Appl. Organomet. Chem.* **2022**, e6982. [[CrossRef](#)]
29. Li, P.; Sun, L.; Xue, S.; Qu, D.; An, L.; Wang, X.; Sun, Z. Recent advances of carbon dots as new antimicrobial agents. *Smartmat* **2022**, *3*, 226–248. [[CrossRef](#)]

30. Ndayishimiye, J.; Kumeria, T.; Popat, A.; Falconer, J.R.; Blaskovich, M.A.T. Nanomaterials: The New Antimicrobial Magic Bullet. *ACS Infect. Dis.* **2022**, *8*, 693–712. [[CrossRef](#)]
31. Birhanu, R.; Afrasa, M.A.; Hone, F.G. Recent Progress of Advanced Metal-Oxide Nanocomposites for Effective and Low-Cost Antimicrobial Activates: A Review. *J. Nanomater.* **2023**, *2023*, 8435480. [[CrossRef](#)]
32. Huang, T.; Li, X.; Maier, M.; O'Brien-Simpson, N.M.; Heath, D.E.; O'Connor, A.J. Using inorganic nanoparticles to fight fungal infections in the antimicrobial resistant era. *Acta Biomater.* **2023**, *in press*. [[CrossRef](#)]
33. Sivagami, M.; Asharani, I. Phyto-mediated Ni/NiO NPs and their catalytic applications—a short review. *Inorg. Chem. Commun.* **2022**, *145*, 110054. [[CrossRef](#)]
34. Ahmad, W.; Bhatt, S.C.; Verma, M.; Kumar, V.; Kim, H. A review on current trends in the green synthesis of nickel oxide nanoparticles, characterizations, and their applications. *Environ. Nanotechnol. Monit. Manag.* **2022**, *18*, 100674. [[CrossRef](#)]
35. Zhao, J.; Tian, Y.; Liu, A.; Song, L.; Zhao, Z. The NiO electrode materials in electrochemical capacitor: A review. *Mater. Sci. Semicond. Process.* **2019**, *96*, 78–90. [[CrossRef](#)]
36. Hou, Y.; Gao, S. Monodisperse nickel nanoparticles prepared from a monosurfactant system and their magnetic properties. *J. Mater. Chem.* **2003**, *13*, 1510–1512. [[CrossRef](#)]
37. Angajala, G.; Radhakrishnan, S. A review on nickel nanoparticles as effective therapeutic agents for inflammation. *Inflamm. Cell Signal.* **2014**, *1*, e271.
38. Bräuer, B.; Vaynzof, Y.; Zhao, W.; Kahn, A.; Li, W.; Zahn, D.R.T.; Fernández, C.D.J.; Sangregorio, C.; Salvan, G. Electronic and magnetic properties of Ni nanoparticles embedded in various organic semiconductor matrices. *J. Phys. Chem. B* **2009**, *113*, 4565–4570. [[CrossRef](#)]
39. Pandian, C.J.; Palanivel, R.; Dhananasekaran, S. Green synthesis of nickel nanoparticles using *Ocimum sanctum* and their application in dye and pollutant adsorption. *Chin. J. Chem. Eng.* **2015**, *23*, 1307–1315. [[CrossRef](#)]
40. Ghosal, A.; Shah, J.; Kotnala, R.K.; Ahmad, S. Facile green synthesis of nickel nanostructures using natural polyol and morphology dependent dye adsorption properties. *J. Mater. Chem. A* **2013**, *1*, 12868–12878. [[CrossRef](#)]
41. Din, M.I.; Nabi, A.G.; Rani, A.; Aihetasham, A.; Mukhtar, M. Single step green synthesis of stable nickel and nickel oxide nanoparticles from *Calotropis gigantea*: Catalytic and antimicrobial potentials. *Environ. Nanotechnol. Monit. Manag.* **2018**, *9*, 29–36. [[CrossRef](#)]
42. Thema, F.; Manikandan, E.; Gurib-Fakim, A.; Maaza, M. Single phase bunsenite NiO nanoparticles green synthesis by *Agathosma betulina* natural extract. *J. Alloy. Compd.* **2016**, *657*, 655–661. [[CrossRef](#)]
43. Vijayakumar, S.; Nagamuthu, S.; Muralidharan, G. Supercapacitor studies on NiO nanoflakes synthesized through a microwave route. *ACS Appl. Mater. Interfaces* **2013**, *5*, 2188–2196. [[CrossRef](#)] [[PubMed](#)]
44. Kim, S.-G.; Yoon, S.P.; Han, J.; Nam, S.W.; Lim, T.H.; Oh, I.-H.; Hong, S.-A. A study on the chemical stability and electrode performance of modified NiO cathodes for molten carbonate fuel cells. *Electrochim. Acta* **2004**, *49*, 3081–3089. [[CrossRef](#)]
45. Jaji, N.-D.; Lee, H.L.; Hussin, M.H.; Akil, H.; Zakaria, M.R.; Othman, M.B.H. Advanced nickel nanoparticles technology: From synthesis to applications. *Nanotechnol. Rev.* **2020**, *9*, 1456–1480. [[CrossRef](#)]
46. Din, M.I.; Rani, A. Recent advances in the synthesis and stabilization of nickel and nickel oxide nanoparticles: A green adeptness. *Int. J. Anal. Chem.* **2016**, *2016*, 3512145. [[CrossRef](#)]
47. Vijayaraghavan, K.; Nalini, S.P.K. Biotemplates in the green synthesis of silver nanoparticles. *Biotechnol. J.* **2010**, *5*, 1098–1110. [[CrossRef](#)]
48. Ghotekar, S. A review on plant extract mediated biogenic synthesis of CdO nanoparticles and their recent applications. *Asian J. Green Chem.* **2019**, *3*, 187–200. [[CrossRef](#)]
49. Van Tran, T.; Nguyen, D.T.C.; Kumar, P.S.; Din, A.T.M.; Jalil, A.A.; Vo, D.-V.N. Green synthesis of ZrO₂ nanoparticles and nanocomposites for biomedical and environmental applications: A review. *Environ. Chem. Lett.* **2022**, *20*, 1309–1331. [[CrossRef](#)]
50. Dabhane, H.; Ghotekar, S.; Zate, M.; Kute, S.; Jadhav, G.; Medhane, V. Green synthesis of MgO nanoparticles using aqueous leaf extract of Ajwain (*Trachyspermum ammi*) and evaluation of their catalytic and biological activities. *Inorg. Chem. Commun.* **2022**, *138*, 109270. [[CrossRef](#)]
51. Bandeira, M.; Giovanela, M.; Roesch-Ely, M.; Devine, D.M.; da Silva Crespo, J. Green synthesis of zinc oxide nanoparticles: A review of the synthesis methodology and mechanism of formation. *Sustain. Chem. Pharm.* **2020**, *15*, 100223. [[CrossRef](#)]
52. Ghotekar, S.; Pagar, K.; Pansambal, S.; Murthy, H.C.A.; Oza, R. Biosynthesis of silver sulfide nanoparticle and its applications. In *Handbook of Greener Synthesis of Nanomaterials and Compounds*; Elsevier: Amsterdam, The Netherlands, 2021; pp. 191–200. [[CrossRef](#)]
53. Ghotekar, S.; Pansambal, S.; Bilal, M.; Pingale, S.S.; Oza, R. Environmentally friendly synthesis of Cr₂O₃ nanoparticles: Characterization, applications and future perspective—A review. *Case Stud. Chem. Environ. Eng.* **2021**, *3*, 100089. [[CrossRef](#)]
54. Singh, J.; Dutta, T.; Kim, K.-H.; Rawat, M.; Samddar, P.; Kumar, P. 'Green' synthesis of metals and their oxide nanoparticles: Applications for environmental remediation. *J. Nanobiotechnol.* **2018**, *16*, 84. [[CrossRef](#)]
55. Marzban, A.; Mirzaei, S.Z.; Karkhane, M.; Ghotekar, S.K.; Danesh, A. Biogenesis of copper nanoparticles assisted with seaweed polysaccharide with antibacterial and antibiofilm properties against methicillin-resistant *Staphylococcus aureus*. *J. Drug Deliv. Sci. Technol.* **2022**, *74*, 103499. [[CrossRef](#)]
56. Khan, F.; Sarker, M.R.; Ming, L.C.; Mohamed, I.N.; Zhao, C.; Sheikh, B.Y.; Tsong, H.F.; Rashid, M.A. Comprehensive review on phytochemicals, pharmacological and clinical potentials of *Gymnema sylvestre*. *Front. Pharmacol.* **2019**, *10*, 1223. [[CrossRef](#)]

57. German Federal Institute for Risk Assessment, Germany; Marakis, G.; Ziegenhagen, R.; Lampen, A.; Hirsch-Ernst, K. Risk assessment of substances used in food supplements: The example of the botanical *Gymnema sylvestre*. *EFSA J.* **2018**, *16*, e16083.
58. Tiwari, P.; Mishra, B.N.; Sangwan, N.S. Phytochemical and Pharmacological Properties of *Gymnema sylvestre*: An Important Medicinal Plant. *BioMed Res. Int.* **2014**, *2014*, 830285. [[CrossRef](#)]
59. Yudasari, N.; Wiguna, P.A.; Handayani, W.; Suliyanti, M.M.; Imawan, C. The formation and antibacterial activity of Zn/ZnO nanoparticle produced in *Pometia pinnata* leaf extract solution using a laser ablation technique. *Appl. Phys. A* **2021**, *127*, 56. [[CrossRef](#)]
60. Ali, T.; Warsi, M.F.; Zulfiqar, S.; Sami, A.; Ullah, S.; Rasheed, A.; Alsafari, I.A.; Agboola, P.O.; Shakir, I.; Baig, M.M. Green nickel/nickel oxide nanoparticles for prospective antibacterial and environmental remediation applications. *Ceram. Int.* **2022**, *48*, 8331–8340. [[CrossRef](#)]
61. Barwant, M.; Ugale, Y.; Ghotekar, S.; Basnet, P.; Nguyen, V.-H.; Pansambal, S.; Murthy, H.C.A.; Sillanpaa, M.; Bilal, M.; Oza, R.; et al. Eco-friendly synthesis and characterizations of Ag/AgO/Ag₂O nanoparticles using leaf extracts of *Solanum elaeagnifolium* for antioxidant, anticancer, and DNA cleavage activities. *Chem. Pap.* **2022**, *76*, 4309–4321. [[CrossRef](#)]
62. García-Cerda, L.; Bernal-Ramos, K.; Montemayor, S.M.; Quevedo-López, M.; Betancourt-Galindo, R.; Bueno-Báques, D. Preparation of hcp and fcc Ni and Ni/NiO nanoparticles using a citric acid assisted pechini-type method. *J. Nanomater.* **2011**, *2011*, 72. [[CrossRef](#)]
63. Kadam, J.; Madiwale, S.; Bashte, B.; Dindorkar, S.; Dhawal, P.; More, P. Green mediated synthesis of palladium nanoparticles using aqueous leaf extract of *Gymnema sylvestre* for catalytic reduction of Cr (VI). *SN Appl. Sci.* **2020**, *2*, 1854. [[CrossRef](#)]
64. Subashini, M.; Rajendran, P.; Ashok, G.; Kanthesh, B. TLC, FTIR and GCMS analysis of leaves of *Gymnema sylvestre* R. Br from Kolli Hills, Tamil Nadu, India. *Int. J. Curr. Microbiol. App. Sci.* **2015**, *4*, 757–764.
65. Wang, T.; Lin, J.; Chen, Z.; Megharaj, M.; Naidu, R. Green synthesized iron nanoparticles by green tea and eucalyptus leaves extracts used for removal of nitrate in aqueous solution. *J. Clean. Prod.* **2014**, *83*, 413–419. [[CrossRef](#)]
66. Sabouri, Z.; Fereydouni, N.; Akbari, A.; Hosseini, H.A.; Hashemzadeh, A.; Amiri, M.S.; Oskuee, R.K.; Darroudi, M. Plant-based synthesis of NiO nanoparticles using salvia macrosiphon Boiss extract and examination of their water treatment. *Rare Met.* **2020**, *39*, 1134–1144. [[CrossRef](#)]
67. Kumari, L.; Li, W.Z.; Vannoy, C.; Leblanc, R.M.; Wang, D.Z. Vertically aligned and interconnected nickel oxide nanowalls fabricated by hydrothermal route. *Cryst. Res. Technol. J. Exp. Ind. Crystallogr.* **2009**, *44*, 495–499. [[CrossRef](#)]
68. Gandhi, A.C.; Wu, S.Y. Strong deep-level-emission photoluminescence in NiO nanoparticles. *Nanomaterials* **2017**, *7*, 231. [[CrossRef](#)]
69. Suresh, S.; Karthikeyan, S.; Saravanan, P.; Jayamoorthy, K. Comparison of antibacterial and antifungal activities of 5-amino-2-mercaptobenzimidazole and functionalized NiO nanoparticles. *Karbala Int. J. Mod. Sci.* **2016**, *2*, 188–195. [[CrossRef](#)]
70. Ahmad, B.; Khan, M.; Naeem, M.; Alhodaib, A.; Fatima, M.; Amami, M.; Al-Abbad, E.A.; Kausar, A.; Alwadai, N.; Nazir, A.; et al. Green synthesis of NiO nanoparticles using Aloe vera gel extract and evaluation of antimicrobial activity. *Mater. Chem. Phys.* **2022**, *288*, 126363. [[CrossRef](#)]
71. Ezhilarasi, A.A.; Vijaya, J.J.; Kaviyarasu, K.; Kennedy, L.J.; Ramalingam, R.J.; Al-Lohedan, H.A. Green synthesis of NiO nanoparticles using *Aegle marmelos* leaf extract for the evaluation of in-vitro cytotoxicity, antibacterial and photocatalytic properties. *J. Photochem. Photobiol. B Biol.* **2018**, *180*, 39–50. [[CrossRef](#)]
72. Huq, A.; Ashrafudoulla; Rahman, M.M.; Balusamy, S.R.; Akter, S. Green synthesis and potential antibacterial applications of bioactive silver nanoparticles: A review. *Polymers* **2022**, *14*, 742. [[CrossRef](#)]

Disclaimer/Publisher’s Note: The statements, opinions and data contained in all publications are solely those of the individual author(s) and contributor(s) and not of MDPI and/or the editor(s). MDPI and/or the editor(s) disclaim responsibility for any injury to people or property resulting from any ideas, methods, instructions or products referred to in the content.